Phase Transitions and Crystal Structures of Ionic Plastic Crystals Comprising Quaternary Ammonium Cations and Carborane Anion

Kimata, Hironori
Sumitani, Ryo
Mochida, Tomoyuki

(Citation)
Chemistry Letters,48(8):859-862

(Issue Date)
2019-08

(Resource Type)
journal article

(Version)
Accepted Manuscript

(URL)
https://hdl.handle.net/20.500.14094/90006332

Phase Transitions and Crystal Structures of Ionic Plastic Crystals Comprising Quaternary Ammonium Cations and Carborane Anion

Hironori Kimata,[1] Ryo Sumitani,[1] and Tomoyuki Mochida*[1,2]
[1]*Department of Chemistry, Graduate School of Science, Kobe University, Rokkodai, Nada, Kobe, Hyogo 657-8501*
[2]*Center for Membrane and Film Technology, Kobe University, Rokkodai, Nada, Kobe, Hyogo 657-8501*

E-mail: tmochida@platinum.kobe-u.ac.jp

Quaternary ammonium salts with the carborane anion $CB_{11}H_{12}^-$ ([cation][$CB_{11}H_{12}$]; cations : Me_4N^+, Et_4N^+, $(C_4H_8)_2N^+$, Bu_4N^+, and $MeEt_3(MeOCH_2CH_2)N^+$) were prepared. Each salt displayed several solid phase transitions and exhibited an ionic plastic phase at high temperatures. Crystallographic analysis revealed that the disorder of the cation conformation and anion orientation become more extensive in the higher temperature phases.

Keywords: Ionic plastic crystals, Phase transitions, Carborane

Organic ionic plastic crystals are useful as solid-state electrolytes owing to their high ionic conductivity.[1,2] Onium cations have been extensively used in the design and synthesis of organic ionic plastic crystals over the last decade.[3,4] The plastic phase is often exhibited by solids containing globular molecules that exhibit orientational or rotational disorder, and as a consequence of the disorder, plastic crystals often display a small entropy of fusion (ΔS < 20 J K^{-1} mol^{-1}) and exhibit highly symmetric crystal structures with a cubic or hexagonal lattice.[5] Organic ionic plastic crystals often exhibit successive phase transitions from an ordered crystalline phase to orientationally disordered phases.[2-4]

We report, herein, the phase transitions and crystal structures of several quaternary ammonium salts with the $CB_{11}H_{12}$ anion (cations: Me_4N^+, Et_4N^+, $(C_4H_8)_2N^+$, Bu_4N^+, and $MeEt_3(MeOCH_2CH_2)N^+$ (DEME); Figure 1). The $CB_{11}H_{12}$ anion is a stable, weakly coordinating carborane anion with an icosahedral geometry.[6] Only a few ionic plastic crystals with carborane anions have been reported,[7] despite their extensive use in ionic liquids.[8,9] We were interested in the phase transitions of salts with such globular anions.

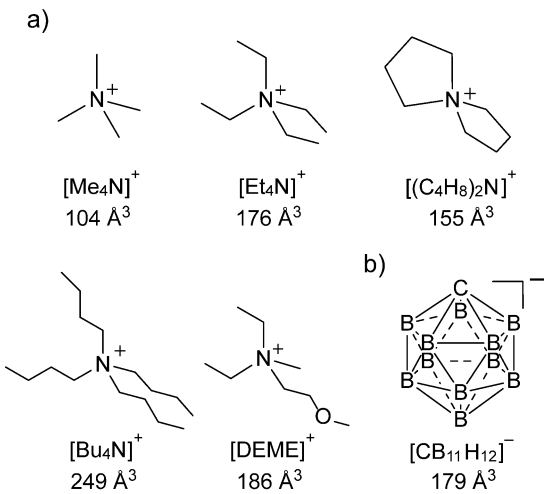

Figure 1. Structural formulae of the (a) quaternary ammonium cations and (b) carborane anion used in this study. The van der Waals volumes of the molecules are shown beneath each structure.

The phase behaviors of the prepared salts were investigated by differential scanning calorimetry (DSC).[10] All salts exhibited two or three solid phase transitions (Figure 2), and their highest temperature solid phase (phase I) is regarded as a plastic phase, which is indicated by the loss of birefringence observed using polarized optical microscopy, the formation of the cubic crystal lattice, and the rather small melting entropies for the Bu_4N and DEME salts, all of which are a consequence of reorientation of the molecules. The phase transitions to phase I occurred between 344–496 K. Interestingly, the transition temperatures were similar to those of $[NR_4][PF_6]$[3b] (545 K, 338 K, and 360 K, for R = Me, Et, and Bu, respectively), despite the large difference in anion size. Phase II of the Me_4N salt may also be regarded as a plastic phase because it exhibited a cubic lattice structure and a very small transition entropy to phase I ($\Delta S_{II\text{-}I}$ = 2.4 J K^{-1} mol^{-1}). The Et_4N and $(C_4H_8)_2N$ salts have comparable cation size, whereas the

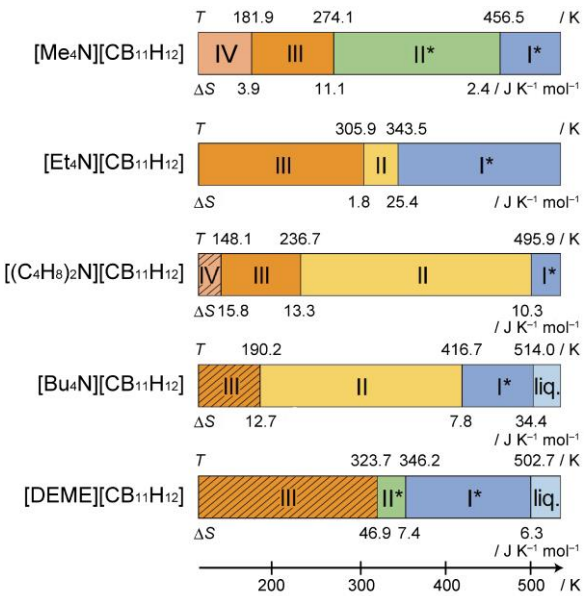

Figure 2. Phase diagrams of [cation][$CB_{11}H_{12}$]. The phase transition temperature (K) and the phase transition entropy (J K^{-1} mol^{-1}) are shown above and below each bar chart, respectively. The asterisks represent orientationally disordered phases. The areas with diagonal lines are fully ordered phases.

latter salt had a very high transition temperature to the plastic phase (T_C = 495.9 K). This is likely due to the rigid, non-globular shape of the $(C_4H_8)_2N$ cation. In addition, the packing coefficient of the $(C_4H_8)_2N$ salt (68.2% at 100 K) was higher than those of other salts (65.4–66.4%).

The Bu_4N and DEME salts exhibited melting at 514.0 K (ΔS_m = 34.4 J K^{-1} mol^{-1}) and 502.7 K (ΔS_m = 6.3 J K^{-1} mol^{-1}), respectively, whereas other salts decomposed before melting. The decomposition temperatures of the salts in Figure 2 determined by thermogravimetric analysis (−5wt%, 10 K min^{-1}) were 682, 634, 662, 589, and 598 K, respectively. They are close to those of the corresponding PF_6 salts.[3b] The melting entropy of the Bu_4N salt was higher than 20 J K^{-1} mol^{-1}, but such a relatively large entropy can be observed in organic ionic plastic crystals.[2] In the DEME salt, the sum of $\Delta S_{II\text{-}I}$ (7.4 J K^{-1} mol^{-1}) and ΔS_m (6.3 J K^{-1} mol^{-1}) is lower than 20 J K^{-1} mol^{-1}, which indicates that phase II is also an orientationally disordered phase. Considering its anisotropic crystal lattice observed by powder X-ray diffraction measurements, phase II is probably a rotator phase.

The structures of the plastic phases were investigated by powder X-ray diffraction measurements. The analysis of the diffraction patterns indicated that $[Me_4N][CB_{11}H_{12}]$ (phase II), $[Et_4N][CB_{11}H_{12}]$ (phase I), and [DEME][$CB_{11}H_{12}$] (phase I) have a CsCl-type structure, though the peaks were less clear in [DEME][$CB_{11}H_{12}$]. Their lattice constants were determined to be 7.12, 7.81, and 7.96 Å, respectively, and the interionic distances derived from them agreed well with the sum of Van der Waals radii estimated from DFT calculations (Table 1). The radius ratio ($\rho = r_{small\ ion}/r_{large\ ion}$) calculated using the ionic radii were in

Table 1. Lattice constants, interionic distances, and radius ratios in the high-temperature phases.

Salts	Temperature (K)	Lattice constants (Å)	Interionic distance (Å)	Radius ratio[a]
$[Me_4N][CB_{11}H_{12}]$	343 (Phase II)	7.12	6.16 (6.41[a])	0.84
$[Et_4N][CB_{11}H_{12}]$	363 (Phase I)	7.81	6.76 (6.97[a])	1.00
[DEME][$CB_{11}H_{12}$]	363 (Phase I)	7.96	6.89 (7.03[a])	0.99

a) Estimated by DFT calculations.

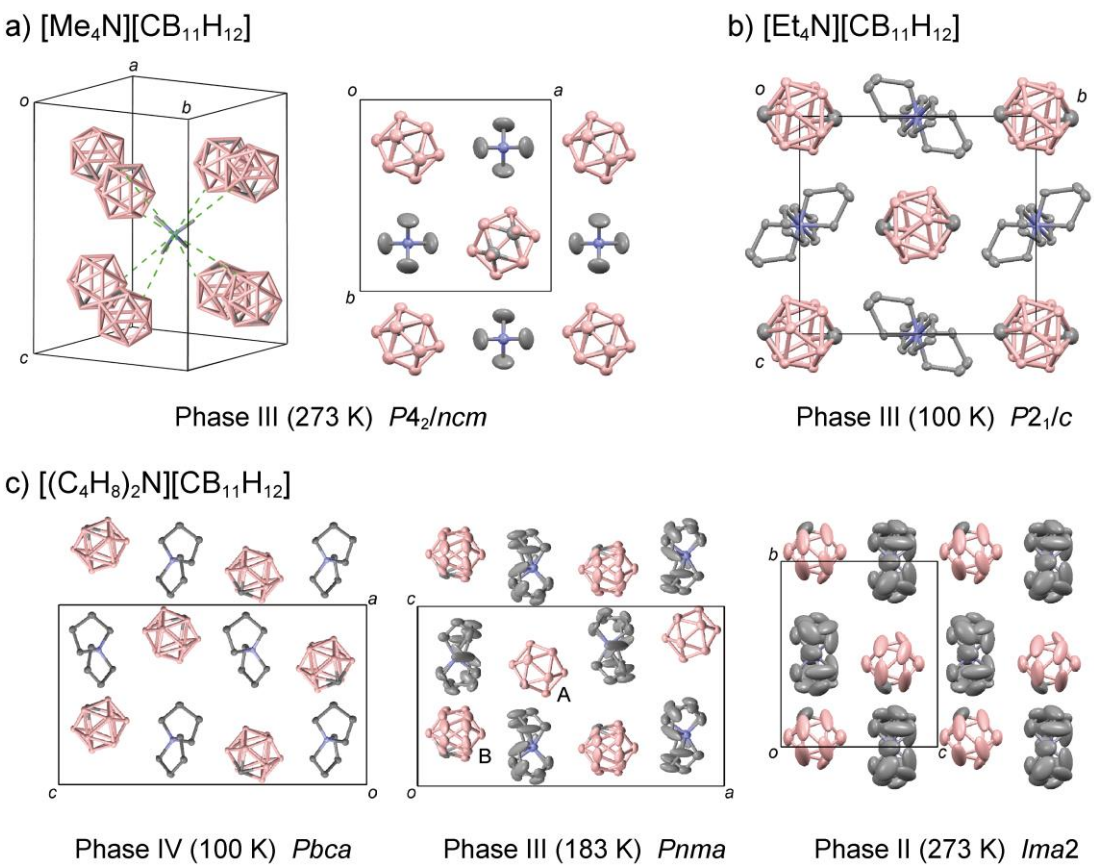

Figure 3. Packing diagrams of [cation][$CB_{11}H_{12}$] (Cation: (a) Me_4N, (b) Et_4N, and (c) $(C_4H_8)_2N$). The dashed lines in figure (a) (left) are merely guides. The hydrogen atoms have been omitted for clarity.

the range of 0.84–1.00. These results are in agreement with the radius ratio rule in inorganic ion crystals, which predicts an eight-coordinated structure for crystals with $\rho > 0.73$.[7]

Single crystal X-ray structure analysis was performed for all non-plastic phases.[11] In all salts, the cations and anions were arranged alternately, exemplified by the packing diagram of the Me_4N salt (phase III) shown in Figure 3a (left). The coordination number, which is the number of anions surrounding a cation and vice versa, was eight, for all salts except the Bu_4N salt, for which the coordination number was not clear due to the presence of the alkyl chains. The cations and anions were ordered in the lowest temperature phase in most of the salts (areas with diagonal lines in Figure 2). In these phases, the C–B bonds (~1.72 Å) in the anion were shorter than the B–B bonds (~1.77 Å), and the molecular skeleton is distorted from an ideal icosahedral geometry, in accordance with the literature data.[10] The anion in the other phases was disordered in most cases and exhibited averaged bond lengths. The disorder of the cation and anion in each salt became more extensive in the higher temperature phases.

The packing diagrams of the Me_4N salt in phase III (273 K) are shown in Figure 3a. The structure has a tetragonal unit cell (space group $P4_2/ncm$, $Z = 4$) containing one-fourth of the cation and anion. The Et_4N salt in phase III (100 K) exhibited similar molecular arrangements (Figure 3b). In this phase ($P2_1/c$, $Z = 2$), both the cation and anion are located on inversion centers. All ethyl groups were disordered over two sites with an occupancy of 0.5:0.5. The C atom in the anion was disordered over two adjacent sites and was scrambled by the B atom with an occupancy of 0.5:0.5. The structure in phase II (318 K) was similar to that in phase III and had the same unit cell with the same space group. However, the bond lengths in the anion were observed to be averaged (~1.76 Å), indicating that the C and B atoms were scrambled over the 12 sites. The crystal structures of this salt are similar to that of [Et_4N][7-$SeB_{10}H_{11}$] which has an extensive disorder.[12]

The packing diagrams of the $(C_4H_8)_2N$ salt in phase IV (100 K), phase III (183 K), and phase II (273 K) indicate orthorhombic unit cells for the salt (Figure 3c**)**. Phase IV (*Pbca*) and III (*Pnma*) had similar molecular arrangements and unit cell volumes ($Z = 8$). The cation and anion in phase IV were both ordered, with the cation displaying a twisted structure. However, both the cation and anion were disordered in phase III. One of the two crystallographically independent anions displayed a disorder in which the C atom was disordered over two adjacent sites (anion A, in Figure 3c, middle), while the other anion had an extensive two-fold rotational disorder around a C_5 axis with an occupancy of 0.5:0.5 (anion B). The cation exhibited a two-fold disorder of both five-membered rings with an occupancy of 0.6:0.4. The space group of phase II was *Ima*2, and its unit cell volume was half that of the lower temperature phases ($Z = 4$). The very large, elongated thermal ellipsoids indicate extensive molecular motion. We refrain from a detailed discussion of the structure owing to the low quality of the data due to disorder ($R_1 = 14.7\%$).

The packing diagrams of the Bu_4N salt in phase IV (100 K) and phase III (223 K) are shown in Figure 4a and have monoclinic ($P2_1/n$) and orthorhombic (*Pbca*) unit cells, respectively. The unit cell volume in the latter phase ($Z = 8$) was twice that of the former ($Z = 4$). The anions form pairs exhibiting mutual contacts in phase IV, though the arrangements in phase III were more uniform. The butyl groups in the cation were ordered in phase IV, with two groups existing in the all-*trans* conformation, while the other two exist in a gauche conformation. However, all butyl groups in phase III are disordered over two sites with an occupancy of 0.5:0.5. The packing diagram of the DEME

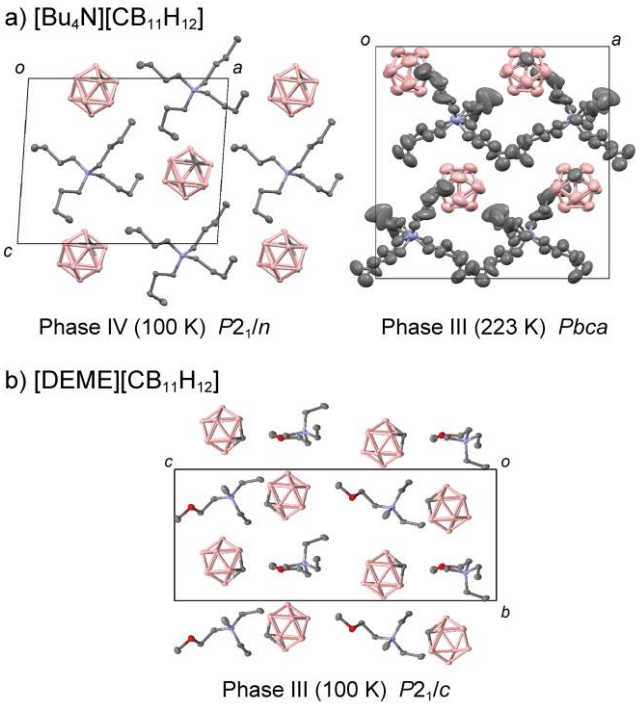

Figure 4. Packing diagrams of [cation][$CB_{11}H_{12}$] (Cation: (a) Bu_4N and (b) DEME). The hydrogen atoms have been omitted for clarity.

salt in phase III (100 K) is also shown in Figure 4b ($P2_1/c$, $Z = 8$). The asymmetric unit contains two pairs of cations and anions.

In summary, the phase behaviors of quaternary ammonium salts with the $CB_{11}H_{12}$ anion were elucidated. Orientational disorder of the anion and conformational disorder of the cation were enhanced successively at the phase transitions. Although this study mainly focused on the structural aspects of the phase transitions, an investigation by NMR spectroscopy is currently underway in our laboratories to elucidate their dynamic features.

This work was supported financially by KAKENHI (18H04516 and 16H04132) from the Japan Society for the Promotion of Science (JSPS).

Supporting information is available at http://dx.doi.org/10.1246/cl.****

References and Notes

1 D.R. MacFarlane, J. Huang, M. Forsyth, *Nature*, **1999**, *402*, 792.

2 H. Zhu, D. R. MacFarlane, J. M. Pringle, M. Forsyth, *Trends Chem*. **2019**, *1*, 126.

3 a) Z.B. Zhou, H. Matsumoto, *Electrochem. Commun*. **2007**, *9*, 1017. b) K. Matsumoto, U. Harinaga, R. Tanaka, A. Koyama, R. Hagiwara, K. Tsunashima, *Phys. Chem. Chem. Phys.* **2014**, *16*, 23616. c) M. Yoshizawa-Fujita, E. Kishi, M. Suematsu, T. Takekawa, M. Rikukawa, *Chem. Lett.* **2014**, *43*, 1909.

4 a) T. Hayasaki, S. Hirakawa, H. Honda, *Bull. Chem. Soc. Jpn.* **2013** *86*, 993. b) M. Matsuki, T. Yamada, S. Dekura, H. Kitagawa, N. Kimizuka, *Chem. Lett*. **2018**, ***47***, 497.

5 J. Timmermans, *J. Phys. Chem. Solids*, **1961**, *18*, 1.

6 C. Douvris, J. Michl, *Chem. Rev*. **2013**, *113*, 179.

7 H. Kimata, T. Mochida, *Cryst. Growth Des*. **2018**, *18*, 7562.

8 S. P. Fisher, A. W. Tomich, J. Guo, V. Lavallo, *Chem. Commun.* **2019**, *55*, 1684.

9 a) A. S. Larsen, J. D. Holbrey, F. S. Tham, C. A. Reed, *J. Am. Chem. Soc*. **2000**, *122*, 7264. b) Y. Zhu, N. S. Hosmane, *Eur. J. Inorg. Chem*. **2017**, 4369. c) I. B. Sivaev, *Chem. Heterocycl. Compd.* **2017**, *53*, 638. d) R. M. Dziedzic, M. A. Waddington, S. E. Lee, J. Kleinsasser, J. B. Plumley, W. C. Ewing, B. D. Bosley, V. Lavallo, T. L. Peng, A. M. Spokoyny, *ACS Appl. Mater. Interfaces* **2018**, *10*, 6825. e) M. Kar, O. Tutusaus, D. R. MacFarlane, R. Mohtadi, *Energy Environ. Sci.* **2019**, *12*, 566.

10 The synthetic procedures and DSC traces are provided in the supporting information. The Et_4N salt additionally exhibited a very small irreversible peak (ΔS = 0.5 J K^{-1} mol^{-1}) at 174.0 K in the heating run, but no structural change was observed.

11 The structural analysis for the Me_4N salt in Phase IV was tentative due to twinning, and discussion of the structure was avoided. CCDC-1901232–1901239 and 1907987 contain the crystallographic data for this paper. The crystallographic parameters are provided in the supporting information.

12 D. Reed, G. Ferguson, B. L. Ruhl, O. N. Dhubhghaill, T. R. Spalding, *Polyhedron*, **1988**, ***7***, 17.

Electronic Supporting Information for *Chemistry Letters*

Phase transitions and crystal structures of ionic plastic crystals comprising quaternary ammonium cations and carborane anion

Hironori Kimata,[1] Ryo Sumitani,[1] and Tomoyuki Mochida*[1,2]
[1]*Department of Chemistry, Graduate School of Science, Kobe University, Rokkodai, Nada, Kobe, Hyogo 657-8501*
[2]*Center for Membrane and Film Technology, Kobe University, Rokkodai, Nada, Kobe, Hyogo 657-8501*

Electronic Supporting Information for *Chemistry Letters*

Supporting Information

Contents

Experimental

General. Differential scanning calorimetry (DSC) measurements were performed using a TA Instrument, Q100 differential scanning calorimeter, at a scan rate of 10 K min^{-1}. Thermogravimetric analyses were performed at a heating rate of 10 Kmin^{-1} under a nitrogen atmosphere using a Rigaku TG8120. Bruker APEX II Ultra (MoK□ radiation) was used for single crystal structural analysis and powder X-ray diffraction measurements. SHELXL [S1] was used for structural analysis. The van der Waals volumes of the cations were estimated based on density functional theory calculations (B3LYP/LanL2DZ) using Spartan '18 (Wavefunction, Inc.). Packing coefficients were calculated using PLATON for windows [S2]. Values excluding the NEt_4 salt are shown in the text, as the estimation for the NEt_4 salt was not possible due to the disorder.

[Me_4N][$CB_{11}H_{12}$]. An aqueous solution (0.6 mL) of Cs[$CB_{11}H_{12}$] (38 mg, 0.14 mmol) was added dropwise to an aqueous solution (0.1 mL) of [Me_4N]Cl (28 mg, 0.26 mmol), and was stirred for 30 min. The resulting white precipitate was collected by filtration, and the filtrate was washed several times with ether and dried under vacuum to afford the desired product as a white powder. The product was dissolved in acetonitrile, to which ether was added to prepare a saturated solution. The solution upon standing at −40 ° C for several hours afforded colorless block crystals (5.6 mg, 18% yield). Anal. Calcd. for $C_5H_{24}NB_{11}$: C, 27.65; H, 11.14; N, 6.45. Found: C, 27.84; H, 11.49; N, 6.35.

[Et_4N][$CB_{11}H_{12}$]. An aqueous solution (0.5 mL) of Cs[$CB_{11}H_{12}$] (31 mg, 0.11 mmol) was added dropwise to an aqueous solution (0.2 mL) of [Et_4N]Cl (45 mg, 0.27 mmol), and was stirred for 30 min. The resulting white precipitate was collected by filtration. The filtrate was washed several times with ether and was dried under vacuum to afford the desired product as a white powder. The product was dissolved in dichloromethane and filtered through a short plug of cotton. Ether was slowly diffused into the dichloromethane solution of the product, maintained at -6 °C, over 3 days. The desired product was obtained as white crystals by filtration (24.8 mg, yield 69%). Anal. Calcd. for $C_9H_{32}NB_{11}$: C, 39.56; H, 11.80; N, 5.13. Found: C, 39.46; H, 11.77; N, 5.04.

[Bu_4N][$CB_{11}H_{12}$]. This salt was prepared from [Bu_4N]Cl (25 mg, 0.096 mmol) using Cs[$CB_{11}H_{12}$] (37 mg, 0.14 mmol) by the method as described for [NEt_4][$CB_{11}H_{12}$]. Ether was slowly diffused into an acetone solution of the salt over three days, giving the

desired product as white block crystals (21.8 mg, yield 40%). Anal. Calcd. for $C_{17}H_{48}NB_{11}$: C, 52.97; H, 12.55; N, 3.63. Found: C, 53.19; H, 12.69; N, 3.62.

[DEME][$CB_{11}H_{12}$]. Anion exchange resin (Dowex 1 × 8, chloride form, 7.0 g) was packed in a column, and the column was flushed with a solution of tetrabutylammonium chloride in methanol (50 mM, 50 mL), followed by methanol (100 mL). A solution of [DEME][BF_4] (53 mg, 0.23 mmol) in methanol (2 mL) was applied to the column and eluted with methanol (50 mL). After evaporation of the solvent under reduced pressure, the residue was dried under vacuum to give [DEME]Cl as a colorless liquid. [DEME][$CB_{11}H_{12}$] was synthesized from [DEME]Cl (88 mg, 0.48 mmol) by the same method as described for the synthesis of [Et_4N][$CB_{11}H_{12}$] using Cs[$CB_{11}H_{12}$] (28 mg, 0.10 mmol). Recrystallization was performed from a solvent mixture of ether–dichloromethane by slow cooling (–40 °C), and white needle crystals of the desired product were collected at low temperature (8.0 mg, yield 27%). Anal. Calcd. for $C_9H_{32}NOB_{11}$: C, 37.37; H, 11.15; N, 4.84. Found: C, 37.49; H, 11.45; N, 4.90.

[$(C_4H_8)_2$N][$CB_{11}H_{12}$]. This salt was prepared from [$(C_4H_8)_2$N]Cl (38 mg, 0.23 mmol) by the same method described for [Et_4N][$CB_{11}H_{12}$], using Cs[$CB_{11}H_{12}$] (25 mg, 0.091 mmol). The desired salt was obtained as white needle crystals (8.7 mg, yield 36%) by vapor diffusion of ether into a dichloromethane solution of the salt. Anal. Calcd. for $C_9H_{28}NB_{11}$: C, 40.15; H, 10.48; N, 5.20. Found: C,40.41; H, 10.70; N, 5.09.

[S1] G. M. Sheldrick, *Acta Crystallogr., Sect. A*, 2008, **64**, 112–122.

[S2] A. L. Spek, *Acta Crystallogr., Sect. D*, 2009, **65**, 148–155.

a) $[Me_4N][CB_{11}H_{12}]$

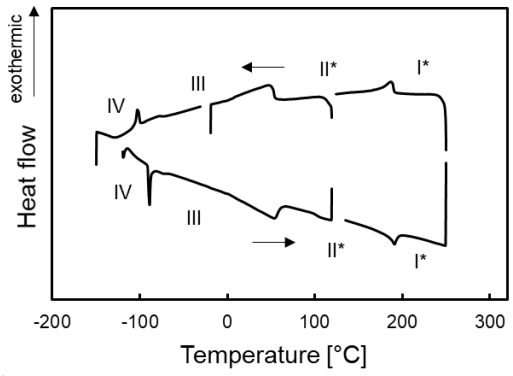

b) $[Et_4N][CB_{11}H_{12}]$

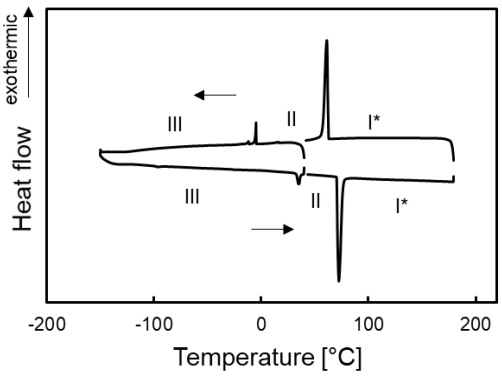

c) $[Bu_4N][CB_{11}H_{12}]$

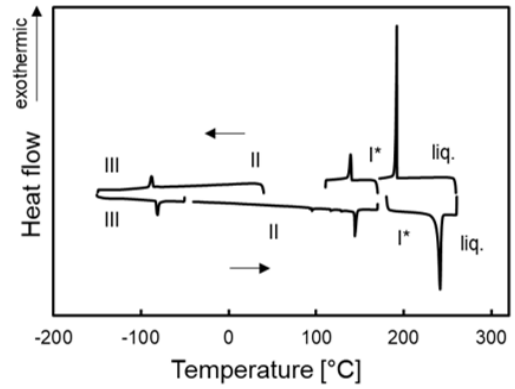

d) $[DEME][CB_{11}H_{12}]$

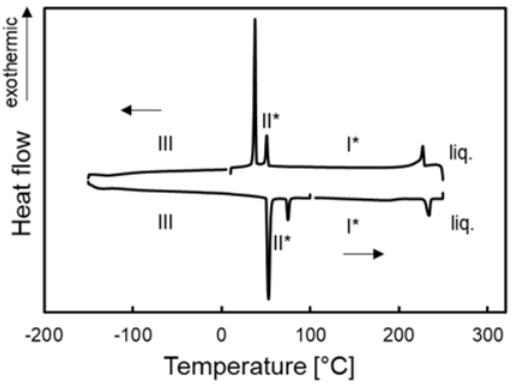

e) $[(C_4H_8)_2N][CB_{11}H_{12}]$

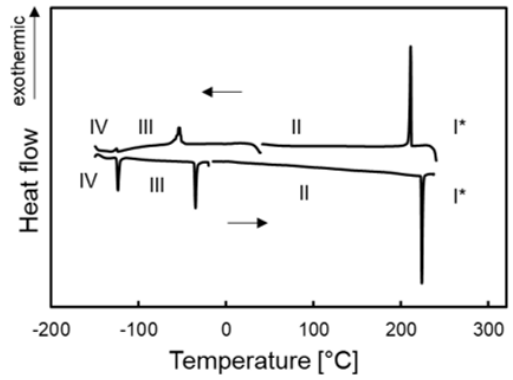

Fig. S1. DSC traces of $[cation][CB_{11}H_{12}]$.

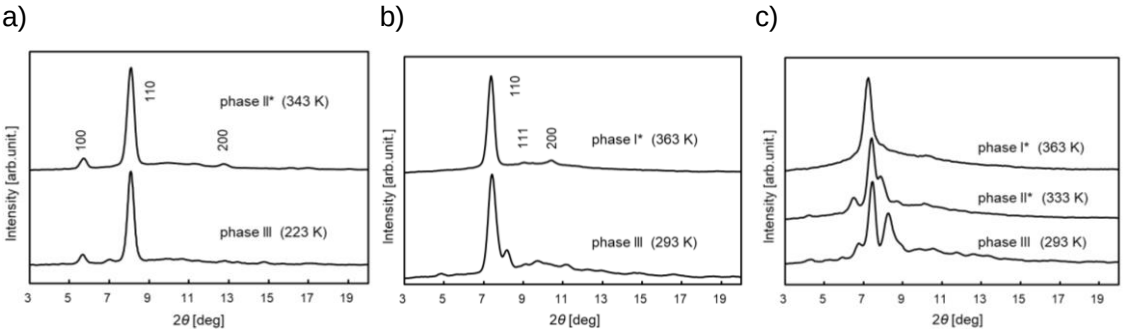

Fig. S2. Powder X-ray diffraction patterns of (a) $[Me_4N][CB_{11}H_{12}]$, (b) $[Et_4N][CB_{11}H_{12}]$, and (c) $[DEME][CB_{11}H_{12}]$ (MoKα radiation).

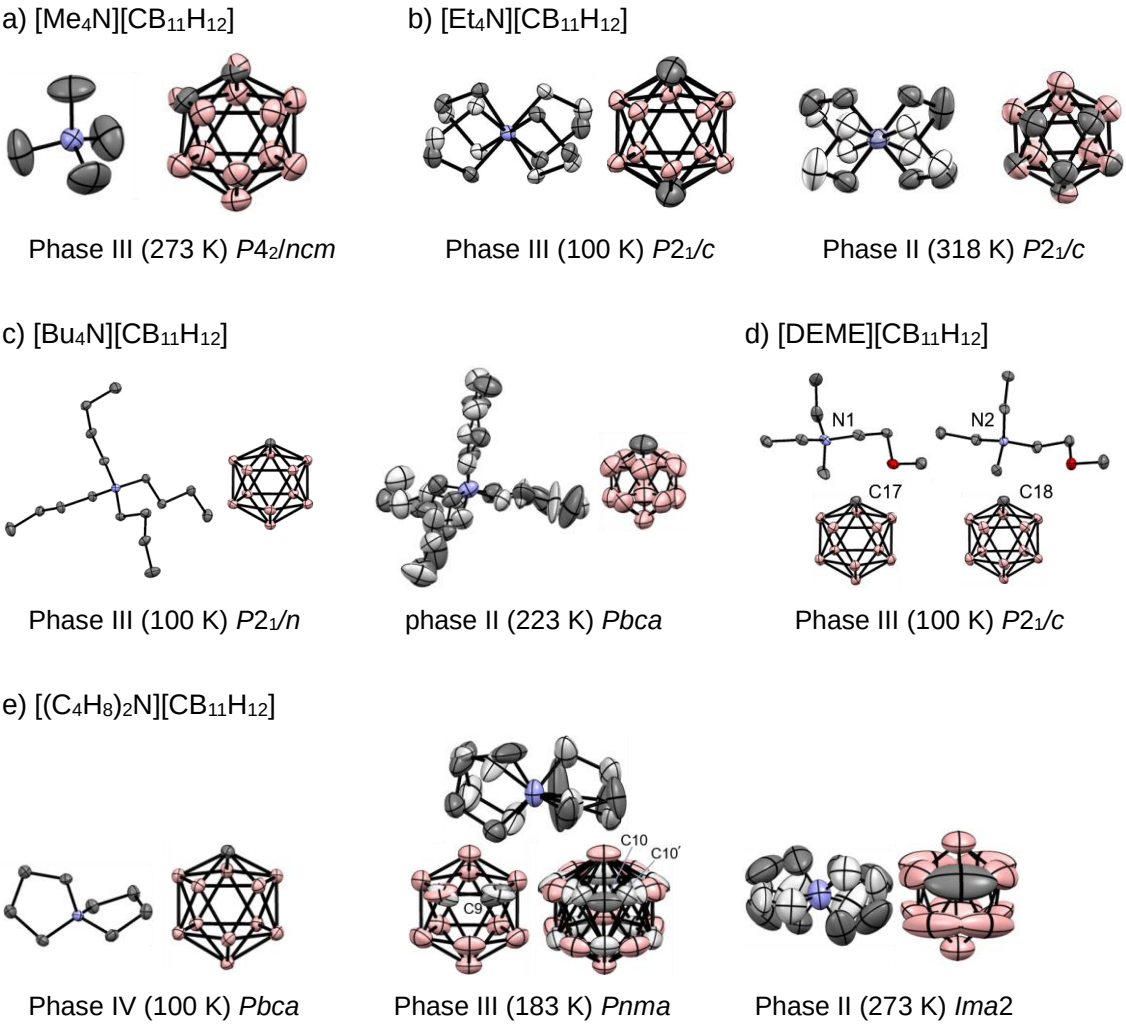

Fig. S3. ORTEP drawings of the cations and anions in $[cation][CB_{11}H_{12}]$. Hydrogen atoms have been omitted for clarity.

Table S1. Crystallographic parameters

	$[Me_4N][CB_{11}H_{12}]$	$[Et_4N][CB_{11}H_{12}]$	
	273 K	100 K	318 K
Empirical formula	$C_5H_{24}B_{11}N$	$C_9H_{32}B_{11}N$	$C_9H_{32}B_{11}N$
Formula weight	217.16	273.26	273.26
Crystal system	Tetragonal	Monoclinic	Monoclinic
Space group	$P4_2/ncm$	$P2_1/c$	$P2_1/c$
a [Å]	10.1481(16)	8.354(6)	8.4755(12)
b [Å]	10.1481(16)	10.598(7)	10.7100(15)
c [Å]	14.079(2)	9.740(6)	10.0671(14)
α [°]	90	90	90
β [°]	90	91.518(8)	91.111(2)
γ [°]	90	90	90
V [Å^3]	1449.9(5)	862.0(10)	913.6(2)
Z	4	2	2
ρ_{calcd} [g cm^{-3}]	0.995	1.053	0.993
F(000)	464	296	296
Reflns collected	7859	4731	5047
Independent reflns	934	1911	2011
Parameters	53	146	187
R(int)	0.0177	0.0203	0.0265
R_1[a], R_w[b] ($I > 2\sigma$)	0.0831, 0.2401	0.0448, 0.1262	0.0619, 0.1693
R_1[a], R_w[b] (all data)	0.0873, 0.2475	0.0465, 0.1288	0.0681, 0.1781
Goodness of fit	1.189	1.063	1.088
$\Delta\rho_{max,min}$ [e Å^{-3}]	0.359, –0.509	0.155, –0.336	0.196, –0.395

[a] $R_1 = \Sigma||F_o| - |F_c|| / \Sigma|F_o|$. [b] $R_w = [\Sigma w (F_o^2 - F_c^2)^2 / \Sigma w (F_o^2)^2]^{1/2}$.

Table S2. Crystallographic parameters

	$[(C_4H_8)_2N][CB_{11}H_{12}]$		
	100 K	183 K	273 K[c]
Empirical formula	$C_9H_{28}B_{11}N$		
Formula weight	269.23		
Crystal system	Orthorhombic	Orthorhombic	Orthorhombic
Space group	*Pbca*	*Pnma*	*Ima*2
a [Å]	11.285(4)	19.727(3)	14.603(5)
b [Å]	14.977(5)	14.691(3)	11.885(6)
c [Å]	19.383(7)	11.535(2)	10.023(3)
α [°]	90	90	90
β [°]	90	90	90
γ [°]	90	90	90
V [Å^3]	3276(2)	3343.0(10)	1739.6(12)
Z	8	8	4
ρ_{calcd} [g cm^{-3}]	1.092	1.070	1.028
F(000)	1152	1152	576
Reflns collected	15884	18439	4813
Independent reflns	3664	3973	1758
Parameters	190	341	142
R(int)	0.0501	0.0342	0.0376
R_1[a], R_w[b] ($I > 2\sigma$)	0.0576, –0.1637	0.0836, 0.2248	0.1474, 0.4257
R_1[a], R_w[b] (all data)	0.0785, –0.1781	0.1001, 0.2419	0.1915, 0.4884
Goodness of fit	1.074	0.984	1.875
$\Delta\rho_{max,min}$ [e Å^{-3}]	0.270, –0.285	0.305, –0.341	0.410, –0.266

[a] $R_1 = \Sigma||F_o| - |F_c|| / \Sigma|F_o|$. [b] $R_w = [\Sigma w (F_o^2 - F_c^2)^2 / \Sigma w (F_o^2)^2]^{1/2}$. [c] The quality of the data was low due to disorder.

Table S3. Crystallographic parameters

	$[Bu_4N][CB_{11}H_{12}]$		$[DEME][CB_{11}H_{12}]$
	100 K	223 K[c]	100 K
Empirical formula	$C_{17}H_{48}B_{11}N$		$C_9H_{32}B_{11}NO$
Formula weight	385.47		289.26
Crystal system	Monoclinic	Orthorhombic	Monoclinic
Space group	$P2_1/n$	*Pbca*	$P2_1/c$
a [Å]	11.445(3)	17.2862(11)	15.505(6)
b [Å]	16.487(4)	17.1973(11)	9.856(4)
c [Å]	13.765(3)	18.0350(11)	24.136(9)
α [°]	90	90	90
β [°]	93.912(3)	90	90.700(5)
γ [°]	90	90	90
V [Å^3]	2591.3(10)	5361.4(6)	3688(2)
Z	4	8	8
ρ_{calcd} [g cm^{-3}]	0.988	0.955	1.042
F(000)	848	1696	1248
Reflns collected	13758	27852	19216
Independent reflns	5654	5551	7947
Parameters	266	415	406
R(int)	0.0249	0.0267	0.0453
R_1[a], R_w[b] ($I > 2\sigma$)	0.0440, 0.1135	0.1000, 0.3304	0.0685, 0.2056
R_1[a], R_w[b] (all data)	0.0528, 0.1196	0.1482, 0.3742	0.0708, 0.2110
Goodness of fit	1.037	1.315	1.057
$\Delta\rho_{max,min}$ [e Å^{-3}]	0.282, –0.243	0.306, –0.149	0.253, –0.491

[a] $R_1 = \Sigma||F_o| - |F_c|| / \Sigma|F_o|$. [b] $R_w = [\Sigma w (F_o^2 - F_c^2)^2 / \Sigma w (F_o^2)^2]^{1/2}$